# *BodyScan*: Enabling Radio-based Sensing on Wearable Devices for Contactless Activity and Vital Sign Monitoring

Biyi Fang‡, Nicholas D. Lane†∗, Mi Zhang‡
Aidan Boran†, Fahim Kawsar†

‡Michigan State University, †Bell Labs, ∗University College London

## ABSTRACT

Wearable devices are increasingly becoming mainstream consumer products carried by millions of consumers. However, the potential impact of these devices is currently constrained by fundamental limitations of their built-in sensors. In this paper, we introduce radio as a new powerful sensing modality for wearable devices and propose to transform radio into a mobile sensor of human activities and vital signs. We present *BodyScan*, a wearable system that enables radio to act as a single modality capable of providing whole-body continuous sensing of the user. BodyScan overcomes key limitations of existing wearable devices by providing a contactless and privacy-preserving approach to capturing a rich variety of human activities and vital sign information. Our prototype design of BodyScan is comprised of two components: one worn on the hip and the other worn on the wrist, and is inspired by the increasingly prevalent scenario where a user carries a smartphone while also wearing a wristband/smartwatch. This prototype can support daily usage with one single charge per day. Experimental results show that in controlled settings, BodyScan can recognize a diverse set of human activities while also estimating the user's breathing rate with high accuracy. Even in very challenging real-world settings, BodyScan can still infer activities with an average accuracy above 60% and monitor breathing rate information a reasonable amount of time during each day.

## Keywords

Wearables; Radio-based Sensing; Channel State Information (CSI); Activity Recognition; Vital Signs

## 1. INTRODUCTION

Wearable devices are growing in popularity at a tremendous rate. The global market of wearable devices is expected to reach a value of 19 billion U.S. dollars in 2018, which is more than ten times its value five years prior [11]. Today, millions of people wear fitness trackers such as Fitbit on a daily basis to track steps, calories burned and sleep [5]. Apple, Google, and Samsung release smartwatches which provide an alternative interface for people to get no-

tifications, respond to text messages, and make phone calls while keeping their smartphones inside pockets [3, 1, 10].

We envision that wearable devices could have a much broader impact on our daily lives beyond tracking steps and sleep as well as being an alternative interface of smartphones. Unfortunately, a key bottleneck that limits their impact is the constraints of the built-in sensors in existing wearable devices. Specifically, IMUs (i.e., accelerometers and gyroscopes) can only sense motions and rotations of body parts to which they are attached. As such, it requires users to wear multiple IMUs to capture whole-body movements. Microphones and image sensors can sense rich information but at the same time they also capture privacy-sensitive data that may cause severe privacy concerns. Physiological sensors such as respiration and ECG sensors are intrusive in that they must be placed at certain body locations and require tight skin contact to function. Motivated by those limitations, *this work is aimed at pushing the boundaries of wearable devices by exploring new sensing modalities that are contactless and privacy-preserving while still being able to provide rich information about users and their context.*

In recent years, radio-based sensing systems have drawn considerable attention because they provide a contactless and privacy-preserving approach to monitor a variety of human activities such as walking [50], cooking [49] and falling [19] as well as vital signs such as breathing and heartbeats [14, 31, 51]. These systems utilize radio transmitters and receivers that are deployed in the ambient environment. However, due to their dependence on the ambient wireless infrastructure, these infrastructure-based systems have three key limitations. First, they can only capture activities and vital signs when people are in the area covered by the ambient wireless infrastructure. Second, their sensing performance degrades when ambient environment changes (e.g., new or moved furniture) or the distance between radio transmitters/receivers and the person being monitored increases. Third, when there is more than one person in the monitored area, activities performed by different individuals interfere with each other, making robust activity recognition extremely challenging.

In this paper, we introduce *BodyScan*, a novel wearable sensing system that uses radio as a single sensing modality for continuous human activity and vital sign monitoring. BodyScan overcomes the aforementioned limitations of infrastructure-based systems. Specifically, BodyScan utilizes radio transmitter and receiver in the form of wearables. As such, it does not require the support of ambient wireless infrastructure and thus enables continuous and ambulatory human activity and vital sign monitoring in all indoor, in-vehicle, and outdoor scenarios. In addition, the wearable radio transmitter and receiver are always within close proximity to the user. As a result, the interference caused by the ambient environment as well as activities performed by surrounding people are

dwarfed by the activity performed by the user, making BodyScan robust to various extraneous interference.

BodyScan is designed to emulate an increasingly prevalent scenario where a user carries a smartphone while wearing a wristband or a smartwatch at the same time. Figure 1 illustrates BodyScan being worn by a user in such scenario. As shown, BodyScan consists of two custom-made wearable devices. One device is a wristband containing a radio transmitter that continuously transmits radio signals. The other device is a wearable unit emulating a smartphone, which is worn on the hip containing a radio receiver that continuously receives radio signals. With the prevalence of smartphones and the increasing popularity of wristbands and smartwatches, we envision that this scenario will become more and more common in the near future. As such, we believe our design has the potential to be widely accepted by the general public.

Based on the design, BodyScan uses radio as a single sensing modality to provide a unified human activity and vital sign sensing solution in the wearable setting. The basic idea of BodyScan is that movements of different parts of the human body caused by different human activities generate different changes on radio signals that are observable at the radio receiver. By analyzing the changes on the received radio signals, the activity that causes the changes can be recognized. To capture the movements of different parts of the human body by just using the wristband and wearable unit, BodyScan uses two custom-designed directional antennas at the radio receiver to track upper body and lower body movements respectively. To analyze the received radio signals, BodyScan exploits the fine-grained Channel State Information (CSI) extracted from the received radio signals, and adopts a tree-structured radio signal processing pipeline that combines upper body and lower body movement information for activity recognition as well as breathing rate estimation. The algorithms involved in the signal processing pipeline are energy-efficient and lightweight to run on resource-constrained wearable platforms in real time.

**Summary of Experimental Results:** We built a lightweight small form-factor prototype of BodyScan and evaluated its performance by conducting experiments in both controlled and uncontrolled settings. With more than 40 hours of data collected from seven subjects, the results of our experiments show that:

- In controlled settings, BodyScan achieves an average classification accuracy of 72.3% for recognizing five most common activities of daily living (ADLs). When the subjects are stationary, it achieves an average accuracy of 97.4% for estimating subjects' breathing rates.

- BodyScan is capable of achieving real-time activity recognition and breathing rate estimation. It can continuously run more than 15 hours, which is sufficient for daily usage with one single charge per day.

- When deployed in the real world, BodyScan achieves an activity recognition accuracy of 60.2% and can opportunistically sense a user's breathing information a reasonable amount of time each day.

**Summary of Contributions:** We introduce the first wearable sensing system that uses only a single pair of on-body radio transmitter and receiver to monitor a wide range of human activities and vital sign in a unified framework. BodyScan takes an *audacious* step towards enabling radio-based sensing on wearable devices. It demonstrates the benefits over existing wearable devices including improved privacy protection by reducing the need for the use of cameras and microphones as well as enhanced comfort and usability by providing a contactless sensing solution and lowering the number
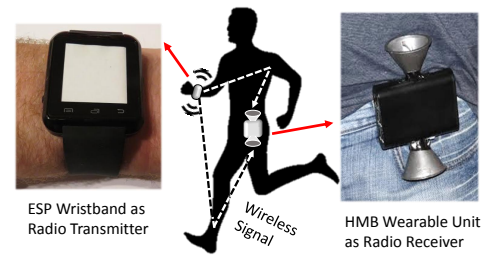


**Figure 1:** The user model of BodyScan. BodyScan consists of two devices: one worn at the wrist and the other worn on the hip. This design choice emulates an increasingly prevalent scenario where a user carries a smartphone while wearing a wristband or a smartwatch at the same time.

of on-body sensors necessary. It also demonstrates the practicality of real-world usage including real-time signal processing as well as long-lasting battery life. Taken together, we believe radio-based wearable sensing systems have tremendous potential to be widely adopted in real world and open up new applications in areas such as mobile health, human-computer interaction, and social computing.

## 2. DESIGN CONSIDERATIONS

In this section, we first describe the design goals that BodyScan aims to achieve. To achieve these goals, BodyScan needs to address a number of challenges. We discuss these challenges and then explain how we tackle these challenges in the design of BodyScan. Based on the design goals, we list the taxonomy of human activities and vital signs which BodyScan aims to capture and recognize.

### 2.1 Design Goals

The following goals are central to the design of BodyScan:

- **Sensing Human Activities and Vital Signs using a Single Sensing Modality:** BodyScan is designed to sense and recognize a wide range of human activities and track vital signs using radio as a *single sensing modality*. Existing wearable sensing systems typically adopt a multimodal sensing approach where more than one sensing modality is employed to capture human activity and vital sign information. For example, physical activities can be sensed by accelerometers while vital signs such as heartbeat can be tracked by a separate pulse oximeter. However, the multimodal sensing approach requires users to wear more than one sensor on different parts of the body, which is a significant burden to users. In contrast, BodyScan aims to capture both human activity and vital sign information using radio only. BodyScan addresses this single sensing modality challenge by noting that both human activity and vital sign information are embedded in the radio signals but they exhibit their unique patterns. Hence, BodyScan utilizes a tree-structured signal processing pipeline that uses different schemes to extract the embedded human activity and vital sign information, respectively.

- **Enabling Whole-Body Sensing with One Pair of Wearable Radio Transmitter/Receiver:** BodyScan is designed to capture *whole-body movements* by using a *single* pair of on-body radio transmitter and receiver. Human activities involve movements from different parts of the body. To capture those movements by using a single pair of on-body radio transmitter and receiver, one straightforward approach is to use omnidirectional antenna at both transmitter and receiver. However, this approach is limited when movements from different parts of the body have similar influences on radio signals. To address this challenge, BodyScan adopts a design that incorporates two directional antennas at the receiver end, with one directional an-
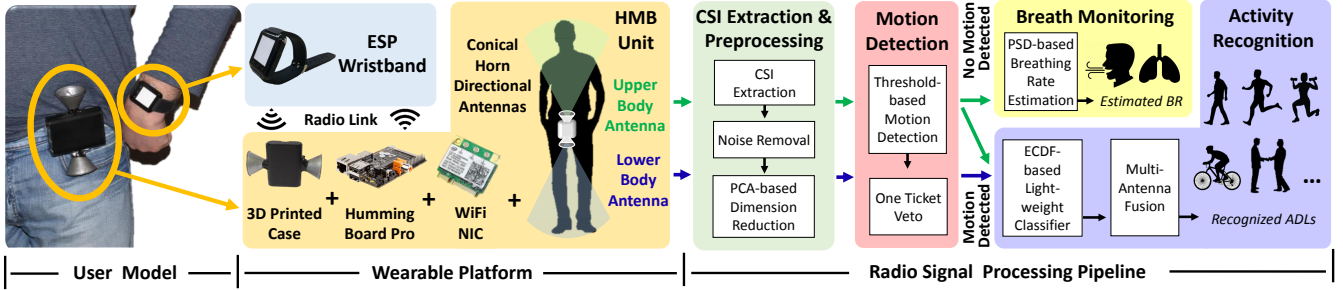
**Figure 2:** The system architecture of BodyScan.

tenna pointing upward to detect upper body movements while the other directional antenna pointing downward to detect lower body movements. BodyScan then combines the upper body and lower body movement information to obtain a complete picture of the whole-body movements. Based on this design, BodyScan achieves a higher resolution so that activities which involve movements from different parts of the body can be better differentiated.

- **Resilient to Noises from Environment and Nearby People:** BodyScan is designed to be *resilient to noises* from ambient environment as well as nearby people. This requires BodyScan to be able to filter out radio signals reflected back from the environment and nearby people. To address this challenge, BodyScan uses conical horn antennas as its directional antennas. Compared to the most commonly used patch antenna, conical horn antenna has a narrower beamwidth, making it more focused on the body areas of the user. As a result, radio reflections caused by ambient environment and nearby people are less likely to be captured by the conical horn antennas, making BodyScan more robust to noises.

- **Operating on Resource-Constrained Platform:** BodyScan is designed to be able to perform *real-time* and *energy-efficient* human activity recognition and vital sign monitoring on resource-constrained wearable platforms. To address this challenge, the tradeoff between computational complexity and real-time/power consumption performance is taken into serious considerations in the design of BodyScan. Specifically, BodyScan adopts a lightweight radio signal processing pipeline to reduce the computational complexity. The pipeline uses Principal Component Analysis (PCA) to reduce the dimensionality of the raw multi-subcarrier CSI measurements; it avoids computationally expensive features and extracts activity information directly from the empirical cumulative distribution function (ECDF) of the radio signals; finally, it utilizes a low computational cost fusion technique that combines movement information from both upper body and lower body to infer the performed activity.

To the best of our knowledge, no existing wearable sensing systems can meet all of the above design goals. This motivates us to design and develop BodyScan to fill this critical gap.

## 2.2 Target Human Activity and Vital Sign

To fully examine the feasibility and explore the potential of our BodyScan system, we have compiled a rich and diverse set of human activities and vital sign based on our design goals. We group them into six different categories which are listed in Table 1. We select these six categories for three main reasons. First, many activities included in the six categories such as *walk*, *brush teeth*, and *type on a keyboard* represent the most common activities performed in our everyday life. Second, the breadth of the considered activ-

| Category | Class |
|---|---|
| Physical Activities (P) | *walk, run* |
| Transportation Mode (T) | *ride a bike, drive a car* |
| Hand-related Activities (H) | *brush teeth, type on a phone, type on a keyboard, shake hands* |
| Free-weight Exercises (E) | *tricep press, front raise, bent-over row, bicep curl, chest fly* |
| Isolated Body (I) Part Movements | *curl left/right arm, swing left/right leg, shake head, bend over* |
| Vital Sign (V) | *breathe* |

**Table 1:** The taxonomy of the target human activity and vital sign.

ities enables us to explore the potential and to have a better understanding of the limitations of radio-based activity recognition in the wearable setting. Specifically, we include activities that involve lower body movements only such as *ride a bike*; upper body movements only such as *shake hands*; whole-body movements such as *run*; as well as isolated body part movements such as *shake head*. Finally, we only include *breathe* in the category of vital sign because we could not reliably detect heart beats and provide accurate heartbeat rate estimation due to the low signal-to-noise ratio (SNR) of the current version of BodyScan.

## 3. BodyScan OVERVIEW

The system architecture of BodyScan is illustrated in Figure 2. As shown, BodyScan consists of a wearable platform as well as a radio signal processing pipeline that runs inside the platform.

The *Wearable Platform* consists of two lightweight small form-factor hardware devices worn on the human body: (1) an ESP wristband (44 x 40 x 8 mm; 35 g) that is designed to be worn on the wrist; and (2) a Hummingboard Pro (HMB) wearable unit (50 x 90 x 140 mm; 200 g) that is designed to be worn on the hip. The ESP wristband acts as the radio transmitter that continuously transmits radio signals while the HMB wearable unit acts as the radio receiver that continuously receives radio signals. In particular, the HMB wearable unit incorporates two conical horn directional antennas, with one detecting the upper body movements (i.e., upper body antenna) and the other detecting the lower body movements (i.e., lower body antenna). Based on this design, BodyScan is able to capture whole-body movements by just using the wristband and the wearable unit.

The *Radio Signal Processing Pipeline* adopts a tree-structured architecture to provide a unified framework for human activity recognition and breath monitoring. At the input, BodyScan extracts multi-subcarrier CSI amplitude measurements from the received packets at both upper and lower body antennas and uses a sliding window to continuously partition the streaming CSI measurements into fixed-length segments. The segment is set to be five seconds
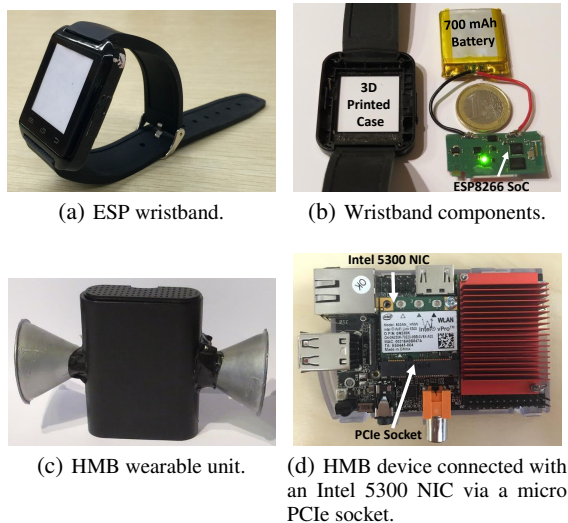
(a) ESP wristband.    (b) Wristband components.



(c) HMB wearable unit.    (d) HMB device connected with an Intel 5300 NIC via a micro PCIe socket.

**Figure 3:** The ESP wristband and HMB wearable unit prototype.

long with 50% overlap. The segmented CSI measurements are processed by the *Preprocessing* module to filter out noises that are not caused by the body movements as well as to extract the most dominant changes that are caused by the body movements. The preprocessed segments from both upper and lower body antennas are then fed into the *Motion Detection* module to identify whether the segments contain upper body or lower body movements caused by human activities. If no movements from both upper and lower body are identified over 15 seconds, the user is determined to be stationary and a power spectral density (PSD)-based scheme is used in the *Breath Monitoring* module to extract the breathing rate information from the 15 seconds CSI measurements of the upper body antenna. Otherwise, the preprocessed segments are fed into the *Activity Recognition* module to be further classified into specific type of the target human activity by fusing upper body and lower body movement information.

In §4 and §5, we describe the design of wearable platform and the radio signal processing pipeline in details.

## 4. WEARABLE PLATFORM

### 4.1 ESP Wristband as Radio Transmitter

Figure 3(a) and 3(b) illustrate the assembled ESP wristband and its individual components respectively. The core component of the ESP wristband is the Espressif ESP8266, a low-power wireless SoC engineered for mobile applications [4]. We connect the ESP8266 to a custom-made small form-factor PCB (35 x 15 mm; 3 g) powered by an external 700 mAH battery. Both the PCB and the battery are housed inside an 3D printed case in the form of a wristband.

The ESP wristband acts as the radio transmitter in our BodyScan system. Radio connection with the HMB wearable unit is established based on the 802.11n protocol over 2.4 GHz band. We program the ESP wristband to operate in WiFi AP host mode and accept wireless connections only from the HMB wearable unit. Once a connection is established, the ESP wristband begins transmitting standard ping packets to the HMB wearable unit continuously. The transmission rate of the ping packets is set to 200 Hz by default.

### 4.2 HMB Wearable Unit as Radio Receiver

Figure 3(c) illustrates the assembled HMB wearable unit. As an overview, the HMB wearable unit consists of two custom-designed

directional antennas attached at the top and bottom of the wearable unit respectively, a Hummingboard Pro (HMB) device [6], and a 5000 mAH battery. The HMB device is a lightweight small form-factor (85 x 56 mm; 78 g) ARM-based mini-computer that contains an on-board 1.2 GHz ARM Cortex-A9 processor. Both the HMB device and the battery are housed inside an 3D printed case that is designed to be attached to the hip of the user.

The HMB wearable unit acts as the radio receiver in our BodyScan system. We connect the HMB device with an Intel WiFi Link 5300 network interface card (NIC) [7] via a micro PCIe socket to collect CSI measurements (see Figure 3(d)). Once the radio connection with the ESP wristband is established, the HMB wearable unit begins receiving wireless packets continuously.

In the following, we describe the details of our custom-designed directional antennas as well as the antenna switching scheme that enables whole-body sensing with one pair of radio transmitter/receiver.

#### 4.2.1 Directional Antenna Design

**Design Rationale:** Different human activities involve movements from different parts of the body. For example, *type on a keyboard* involves hand and finger movements from the upper body; *ride a bike* involves intense leg movements from the lower body; and *run* involves intense arm swings and leg movements from both the upper and lower body. To capture those movements, we adopt a *dual-directional antenna design* by using two conical horn directional antennas and mounting them on the top and bottom of the HMB wearable unit respectively (see Figure 3(c)). When the HMB wearable unit is worn on the hip of the user horizontally, one directional antenna is pointing toward the upper body and the other directional antenna is pointing toward the lower body. As such, the movements of both upper and lower parts of the body can be captured by our HMB wearable unit.

One important design consideration based on our dual-directional antenna design is the radiation angle of the directional antenna. Optimally, our dual-directional antennas should be able to capture all the movements involved in the performed activity from both the upper and lower body. At the same time, they should also be robust to interferences by not capturing radio reflections from ambient environment and nearby people. Figure 4 illustrates this design consideration by showing three scenarios where directional antennas have different radiation angles. Specifically, Figure 4(a) illustrates the scenario where the antenna has a narrow radiation angle. Although a narrow radiation angle is favored in terms of not covering the person spaced with social distance (i.e., 1.2 meters to 2.1 meters [24]), it fails to cover some parts of human body such as shoulders and arms. On the other hand, Figure 4(b) illustrates the scenario where the antenna has a wide radiation angle. Although the wide radiation angle has a full coverage of the whole body, it also covers the nearby people, making the antenna susceptible to interferences. Therefore, a dual-directional antenna design with a radiation angle neither too narrow nor too wide (Figure 4(c)) is desired.

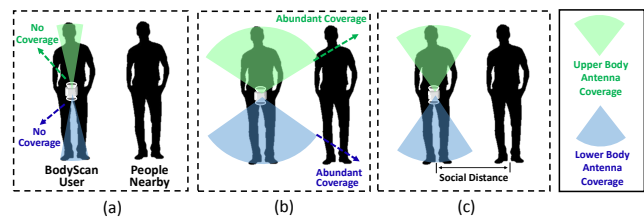**Design Choice and Implementation:** In antenna design, the half-



**Figure 4:** Illustration of three scenarios where directional antennas have different radiation angles.
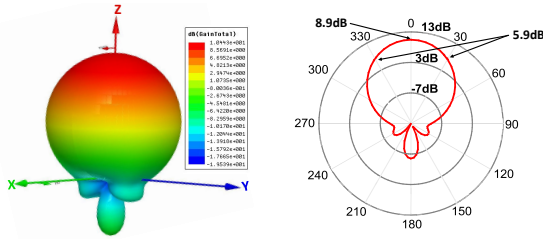
**Figure 5:** Illustration of the simulated radiation patterns of the designed conical horn directional antenna in both 3D space (left) and 2D plane (right). The 3D radiation pattern is characterized by a single main lobe radiated out from the front of the antenna and three back lobes. The 2D plane pattern depicts the elevation plane pattern obtained by slicing through the y-z plane of the 3D radiation pattern. The maximum gain of the designed conical horn directional antenna is 8.9 dB and the HPBW is 60 degrees.

power beamwidth (HPBW) is the metric used to define the radiation angle of an antenna. HPBW is defined as the the angular separation in which the magnitude of the radiation pattern decreases by 50% (i.e., -3.0 dB) from the peak of the main lobe. In our design, the HPBW of our two conical horn directional antennas is set to 60 degrees. As such, when the HMB wearable unit is worn on the hip of the user, the scenario illustrated in Figure 4(c) is achieved.

Based on our design choice, we used the commercial antenna design tool ANSYS HFSS to design and simulate our conical horn directional antenna [2]. Figure 5 illustrates the simulated radiation patterns of our conical horn directional antenna in both 3D space (left) and 2D plane (right). The 3D radiation pattern shown on the left is characterized by a single main lobe radiated out from the front of the antenna and three back lobes. The beamwidths of the main lobe in the azimuth and elevation planes are similar which results in a fairly circular beam. The 2D plane pattern plotted in polar coordinates is shown on the right. It depicts the elevation plane pattern which is obtained by slicing through the y-z plane of the 3D radiation pattern. As shown, the maximum gain of our conical horn directional antenna is 8.9 dB and the HPBW is 60 degrees. Finally, we 3D printed our design to implement our conical horn antennas.

### 4.2.2 Antenna Switching Scheme

Our HMB wearable unit is equipped with two conical horn directional antennas as receiving antennas, with one mounted at the top and the other mounted at the bottom. However, although the Hummingboard Pro device has three on-board antenna interfaces, to reliably receive radio packets, only one antenna interface can be used at one time. To support our dual-directional antenna design, we connect two conical horn directional antennas to two antenna interfaces on the Hummingboard Pro device, and adopt an antenna switching scheme by alternating the access to the two receiving antennas. As such, radio packets can be reliably received at both receiving antennas using one Hummingboard Pro device.

## 5. RADIO SIGNAL PROCESSING PIPELINE

### 5.1 Channel State Information Extraction

Today's wireless devices that support IEEE 802.11a/g/n/ac standards use the Orthogonal Frequency Division Multiplexing (OFDM) as their modulation scheme [21]. An OFDM modulated wireless channel consists of multiple closely spaced narrowband subcarriers at different frequencies. The Channel State Information (CSI) are measurements that describe both the amplitude frequency response as well as the phase frequency response of the wireless channel at the subcarrier level [29]. Compared to the conventionally used Received Signal Strength Indicator (RSSI) that provides a single

measurement of the received signal power averaged over the entire channel, the CSI measurements contain more fine-grained information of the wireless channel.

BodyScan leverages the fine-grained CSI measurements provided by modern wireless devices to capture whole-body movements caused by different activities as well as specific chest movements caused by inhaling and exhaling due to breathing. We installed the modified firmware released by the CSI measurement tool [17] through the Debian Cubox-i Linux OS running on the Hummingboard Pro device at the receiver end, enabling the Intel WiFi Link 5300 NIC to extract CSI measurements from the received packets. Because the CSI phase measurements are reported to be unreliable due to the low-cost hardware components of the commodity wireless devices [37], BodyScan only uses the CSI amplitude measurements for signal processing.

### 5.2 Preprocessing

#### 5.2.1 Noise Removal

The extracted CSI measurements are very noisy in the raw form. It is necessary to filter out the noises before meaningful body movement information can be extracted from the CSI measurements. We observe that the changes of CSI measurements caused by body movements lie at the lower end of the frequency spectrum. Therefore, BodyScan uses a Butterworth low-pass filter on the raw CSI measurements from all the subcarriers to remove high frequency noises that are unlikely to be caused by human body movements. The cut-off frequency of the low-pass filter is set to 20 Hz.

#### 5.2.2 Dimension Reduction

Body movements cause changes on the CSI measurements across all the subcarriers in the wireless channel. As an example, Figure 6 illustrates the CSI amplitude measurements of four different subcarriers from a sample of five-second *walk* activity. There are two key observations that we could obtain from the figure. First, the CSI amplitude measurements across the four subcarriers are highly correlated. Second, different subcarriers have different sensitivity to body movements. Based on these observations, BodyScan utilizes the Principle Component Analysis (PCA) to extract principal components (PCs) from the filtered CSI amplitude measurements across all the subcarriers. The PCs capture the most dominant changes caused by the body movements while removing the redundant information due to the high correlation across subcarriers.

As one of the design goals, BodyScan is designed to be able to operate on resource-constrained wearable platforms. To reduce the computational complexity, only the first PC with the largest
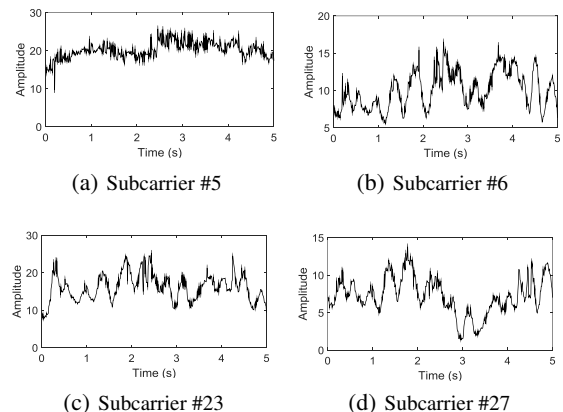


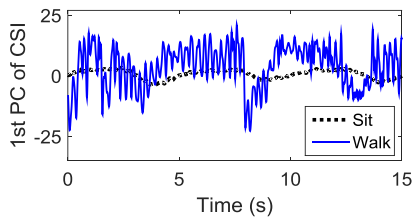**Figure 6:** Correlation and sensitivity differences across subcarriers.

**Figure 7:** First PC of the CSI measurements between *walk* (blue) and *sit on a sofa* (black).
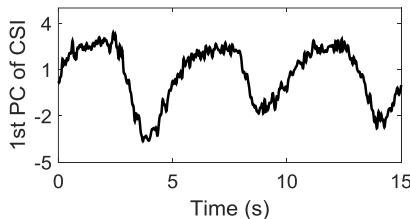


**Figure 8:** Illustration of the first PC of the CSI measurements when the user is stationary.
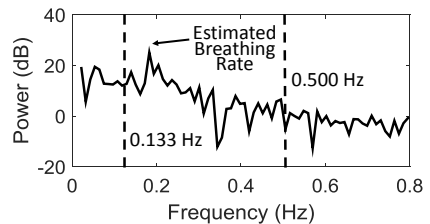


**Figure 9:** The power spectral density (PSD) of breathing.

magnitude of variation is retained in the signal processing pipeline. As such, the high-dimensionality multi-subcarrier CSI amplitude measurements are transformed into a univariate time series.

## 5.3 Motion Detection

The role of the *Motion Detection* module is to detect whether a segment of CSI measurements contains body movements caused by human activities or not. Figure 7 illustrates the first PC of the CSI measurements from *walk* activity and from *sit on a sofa*. Both segments of the CSI measurements are collected from the upper body antenna. We observe that body movements caused by *walk* activity generate much more significant changes on the CSI measurements than *sit on a sofa*. Based on this observation, we define *motion indicator* as the variance of the first PC of the CSI measurements and employ a threshold-based method based on *motion indicator* to determine whether a user is performing some activity or is stationary. Figure 10 shows the values of *motion indicator* of four target human activities (i.e., *walk*, *shake head*, *type on a phone*, and *bent-over row*) as well as being stationary from both upper body antenna (Figure 10(a)) and lower body antenna (Figure 10(b)). As shown, although the values of *motion indicator* of four target human activities vary across a wide range, they are much higher than those of being stationary. Given the data we have collected in this work, we empirically determine the threshold value of *motion indicator* to be 4.3 for upper body antenna and 3.8 for lower body antenna, respectively. Based on these two threshold values, we adopt an *One Ticket Veto* protocol for motion detection. Therefore, a human activity is detected if the *motion indicator* value of either upper or lower body antenna is higher than its corresponding threshold.
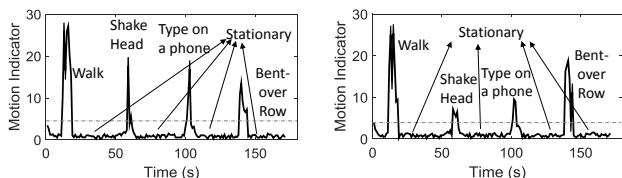


(a) Motion indicator values from upper body antenna.

(b) Motion indicator values from lower body antenna.

**Figure 10:** Illustration of the *motion indicator* values of four human activities and being stationary from upper and lower body antenna, respectively.

## 5.4 Breath Monitoring

To build our *Breath Monitoring* module, we leverage the fact that humans, when stationary (e.g., standing still, watching TV on a sofa), are exhibiting minute and periodic chest movements caused by inhaling and exhaling due to breathing [14, 31, 51]. Figure 8 illustrates the first PC of the CSI measurements collected from the upper body antenna when the user is stationary. As shown, the curve of the first PC presents an evident periodic up-and-down changing pattern over time. This observation indicates that the pe-

riodic chest movements caused by breathing, though minute, can be captured by the first PC of the CSI measurements. Therefore, we harness this fine granularity provided by the CSI measurements to capture those minute and periodic chest movements to estimate a user's breathing rate.

In particular, we use power spectral density (PSD) to extract the breathing rate information from the CSI measurements in the frequency domain [31, 51]. The PSD of the CSI measurements illustrates how power is distributed at each frequency component of the CSI measurements [46]. The rationale behind our PSD-based breathing rate estimation scheme is that the dominant frequency of the chest movements contains the most power across the frequency domain, and the dominant frequency can be used as an estimation of the user's breathing rate. Figure 9 depicts the PSD of the time domain signal illustrated in Figure 8. As shown, there is a strong peak representing the dominant frequency with the power of 26.9 dB at 0.19 Hz, which corresponds to an estimated breathing rate of 11.4 breaths per minute (bpm). This estimated breathing rate is within the range of breathing rates of children, adults and elderly from 8 bpm (0.133 Hz) to 30 bpm (0.5 Hz) [44, 30]. Therefore, when the user is stationary, our breathing rate estimation scheme calculates the PSD of the first PC of CSI measurements over 15 seconds, and determines the user's breathing rate by identifying the highest peak in the PSD within the considered breathing rate range.

## 5.5 Activity Recognition

Our *Activity Recognition* module consists of two components: a lightweight classification scheme based on empirical cumulative distribution function (ECDF) representation and a low computational cost multi-antenna fusion scheme that combines classification results from the upper and lower body antennas.

### 5.5.1 Classification Scheme

One of the design goals of BodyScan is to perform real-time and energy-efficient activity recognition on resource-constrained wearable platforms. To achieve this goal, we purposely avoid computationally expensive features and extract activity information directly from the ECDF of the preprocessed CSI measurements from both upper and lower body antennas. ECDF is able to capture the detailed information of CSI measurement distribution that simple statistical features such as mean or standard deviation can not capture. In addition, because of its low computational cost, ECDF is particularly suitable for resource-constrained wearable platforms [18].

Specifically, the ECDF of activity class $i$ is defined as

$$P_c^{(i)}(x) = P^{(i)}(X \le x) \tag{1}$$

where $x$ covers the whole range of CSI measurement values observed in activity class $i$ and $P_c^{(i)}(x)$ represents the left integral of the distribution of activity class $i$ with value ranging from 0 to 1 [47]. In our ECDF-based classification scheme, we capture the shape of the ECDF curve of activity class $i$ by selecting $d$ points

equally spaced between 0 and 1. For each of those points $p_j$, we derive the value $x_j$ for which $P_c^{(i)}(x_j) = p_j$. Finally, we use these $d$ derived values to construct a $d$-dimension feature vector, and utilize Support Vector Machine (SVM) with probabilistic outputs as the classifier for classification [40].

### 5.5.2 Multi-Antenna Fusion

As the last stage of our signal processing pipeline, given the separate classification results derived from upper and lower body movements respectively, we design a fusion scheme that combines the classification results together to infer the performed activity.

Specifically, let $P_u^{(i)}$ denote the probability of the performed activity classified as class $i$ based on the upper body movements; and $P_l^{(i)}$ denote the probability of the performed activity classified as class $i$ based on the lower body movements. Assuming upper and lower body movements are independent from each other, the probability of the performed activity classified as class $i$ is

$$P_{wholebody}^{(i)} = (P_u^{(i)})^{\frac{var_u}{var_u+var_l}} \cdot (P_l^{(i)})^{\frac{var_l}{var_u+var_l}} \quad (2)$$

where $var_u$ is the variance of CSI measurements collected by upper body antenna and $var_l$ is the variance of CSI measurements collected by lower body antenna. The rationale behind our fusion scheme is that since radio signal variation indicates the occurrence of body movements, higher radio signal variation indicates more movements are involved from a particular body part. As such, the weights assigned to classification probability based on upper and lower body movements are determined by their corresponding radio signal variation ratio. Therefore, the performed activity is classified to the activity class which has the highest $P_{wholebody}$.

## 6. EXPERIMENTAL EVALUATION

We have conducted a set of experiments to evaluate the performance of BodyScan. We break down the whole evaluation into three parts. The first part focuses on benchmarking the performance of BodyScan on activity recognition and breathing rate estimation in controlled settings. We also conduct another four experiments to examine the impact of various factors on the activity recognition performance. These factors include radio frequency interference, interference from nearby people, radio signal transmission rate, and antenna configuration. The second part examines the system performance of BodyScan prototype in terms of runtime performance, power consumption, and battery lifetime. Finally, the third part involves a five-day deployment study that examines the efficacy of BodyScan in real-world settings.

### 6.1 Benchmark Evaluation

#### 6.1.1 Experimental Setup

**Subjects**: We recruited seven subjects (two females) who volunteered to help collect data and conduct evaluation experiments. The subjects are university students and researchers between 25 to 37 ($\mu$ = 29.2) years old, weighted between 49 kg to 82 kg ($\mu$ = 74 kg) and were between 158 cm to 182 cm tall ($\mu$ = 172 cm).

**Experimental Environment**: All the experiments were conducted in controlled settings in both laboratory and outdoor environment. During the experiments, we used WireShark [12] configured in the promiscuous mode to sniff the transmitted packets to monitor the radio frequency interference (RFI) in the environment. To create a clean environment for the subjects to collect radio data using BodyScan, all the wireless devices in the laboratory were turned off. When collecting data in outdoor environment, locations where

RFI was limited were selected. On average, the RFI in the environment during our experiments was 3.3 packets per second (p/s).

**Data and Ground Truth Collection**: Throughout the experiments, the subjects were requested to wear the ESP wristband on the left wrist and the HMB wearable unit on the right hip. To collect activity data, the subjects were instructed to perform the activities listed in Table 1 sequentially. Specifically, the data of *ride a bike*, *drive a car* and *run* was collected in outdoor environment while the data of all other target activities was collected in the laboratory. In the meantime, one researcher acted as an observer to record the ground truth. To collect breathing data, the subjects were instructed to sit still on a chair in the laboratory and breathe naturally. At the same time, the subjects were also asked to wear the NeuLog Respiration Monitor Belt Logger Sensor [9] around the lower ribs to obtain the ground truth measurements of their breathing rates. Figure 14 illustrates this setup. In total, 269 mins of data was collected from all seven subjects and was manually labeled. Table 2 breaks down the amount of data for each of the six categories.

| | Benchmark Evaluation | | | | | | Deployment Study | |
|---|---|---|---|---|---|---|---|---|
| **Type** | P | T | H | E | I | V | Labeled | Unlabeled |
| **Time** | 63m | 43m | 70m | 25m | 36m | 32m | 86m | 2413m |
| **Total** | 269m | | | | | | 2499m | |

**Table 2:** The breakdown of the amount of data collected for benchmark evaluation and deployment study (see Table 1 for data type abbreviations).

#### 6.1.2 Performance of Motion Detection

First, we evaluate the performance of motion detection scheme. As our ground truth, all the data from the categories of P, T, H, E, and I are regarded as *moving* while the data from the category V is regarded as *stationary*. The confusion matrix of motion detection is presented in Table 3. We observe that the true positive rates of both *moving* and *stationary* are very high, indicating that our motion detection scheme can accurately determine whether users are stationary or performing activities in most cases. We also observe that the false positive rate of *moving* is relatively higher than the false positive rate of *stationary*. This is because some target activities such as *type on a keyboard* involve intermediate pauses.

| Ground Truth/Predicted (G/P) | Stationary | Moving |
|---|---|---|
| **Stationary** | 98.2% | 1.8% |
| **Moving** | 7.1% | 92.9% |

**Table 3:** Confusion matrix of motion detection.

#### 6.1.3 Performance of Breathing Rate Estimation

Second, we evaluate the performance of our breathing rate estimation scheme. We collected approximately 32 mins of data in total from all seven subjects. Each subject performs 18 trials of breathing, each lasting for 15 seconds. Figure 11 illustrates the accuracies of estimated breathing rates of all seven subjects. As
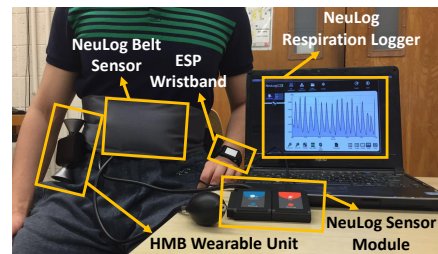


**Figure 14:** Data and ground truth collection for breathing rate estimation.
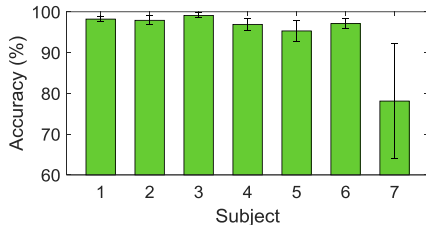
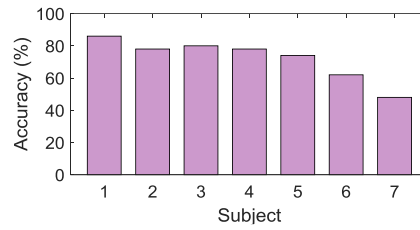**Figure 11:** Breathing rate estimation accuracy.
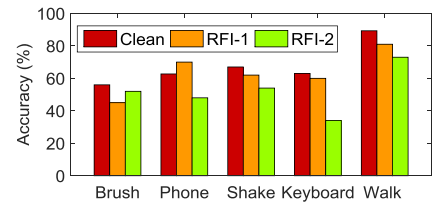


**Figure 12:** Activity recognition accuracy.



**Figure 13:** Impact of RFI.

shown, except Subject 7, the average accuracy of the estimated breathing rates over the other six subjects is 97.4%. This indicates that when the user is stationary, BodyScan is capable of estimating the breathing rate of the user at a very high accuracy despite the differences in gender, age, weight, and height. For Subject 7, the average accuracy drops to 78.1%. This is because during testing, the directional antenna did not point at the upper body of Subject 7 by accident. As such, the directional antenna failed to capture the minute chest movements of Subject 7.

### 6.1.4 Performance of Activity Recognition

**Most Common Activities of Daily Living (ADLs)**: As the first experiment for our activity recognition evaluation, we evaluate the performance of our activity recognition scheme for recognizing five most common activities of daily living (ADLs). These ADLs include *walk*, *brush teeth*, *type on a phone*, *shake hands*, and *type on a keyboard*. We collected a total of 70 mins of data of five most common ADLs from seven subjects. The performance is evaluated using leave-one-subject-out validation.

Figure 12 illustrates the average activity recognition accuracies across five ADLs for all seven subjects. Overall, BodyScan achieves an average recognition accuracy of 72.3% across seven subjects. This result is very promising considering the result is achieved based on the user-independent model. At the same time, we observe that there is a significant difference between the highest (Subject 1) and the lowest (Subject 7) accuracies. This indicates that subjects perform these five ADLs very differently and a personalized model is needed for performance enhancement.

To provide a more detailed view of the result, Table 4 shows the confusion matrix for the five ADLs across seven subjects. We observe that *walk* achieves the best performance in terms of both precision and recall while the other four ADLs have some confusion between each other. This is because *walk* involves intense upper and lower body movements while the other four ADLs only involve hand movements.

| G/P | Brush | Phone | Shake | Keyboard | Walk |
|---|---|---|---|---|---|
| **Brush** | 60.0% | 7.1% | 12.9% | 20.0% | 0.0% |
| **Phone** | 14.3% | 67.1% | 7.1% | 11.4% | 0.0% |
| **Shake** | 15.7% | 8.6% | 71.4% | 4.3% | 0.0% |
| **Keyboard** | 20.0% | 5.7% | 7.1% | 67.1% | 0.0% |
| **Walk** | 1.4% | 0.0% | 1.4% | 1.4% | 95.1% |

**Table 4:** Confusion matrix of Most Common Activities of Daily Living.

**Physical (P) & Transportation (T) & Hand-related (H) Activities**: We then evaluate the performance of our activity recognition scheme for recognizing physical (P), transportation (T) and hand-related (H) activities. These include the aforementioned five most common ADLs and another three activities including *drive a car*, *run* and *ride a bike*. We collected a total of 112 mins of data of the eight activities from seven subjects. The performance is evaluated using leave-one-subject-out validation.

Table 5 shows the confusion matrix for the activities in the P, T, and H categories across seven subjects. Overall, BodyScan achieves an average recognition accuracy of 62.5% across seven subjects. The performance drops compared to the previous ADLs experiment. An important reason accounts for the performance drop is the confusion between *walk* and *run*. As shown in the confusion matrix, almost one third of the *walk* trials are misclassified into *run*. This is because both activities involve intense movements of arms and legs.

| G/P | Brush | Phone | Shake | Keyboard | Walk | Car | Run | Bike |
|---|---|---|---|---|---|---|---|---|
| **Brush** | 63.2% | 0.0% | 10.5% | 15.8% | 10.5% | 0.0% | 0.0% | 0.0% |
| **Phone** | 0.0% | 47.4% | 5.8% | 10.5% | 0.0% | 15.8% | 0.0% | 10.5% |
| **Shake** | 10.5% | 5.3% | 42.1% | 5.3% | 10.5% | 0.0% | 0.0% | 26.3% |
| **Keyboard** | 10.5% | 10.5% | 15.7% | 52.6% | 0.0 % | 10.5% | 0.0% | 0.0% |
| **Walk** | 0.0% | 0.0% | 0.0% | 0.0% | 68.4% | 0.0% | 31.6% | 0.0% |
| **Car** | 5.3% | 0.0% | 5.3% | 0.0% | 10.5% | 73.7% | 5.3% | 0.0% |
| **Run** | 0.0% | 0.0% | 0.0% | 0.0% | 21.1% | 0.0% | 78.9% | 0.0% |
| **Bike** | 5.3% | 5.3% | 10.5% | 0.0% | 0.0% | 0.0% | 5.3% | 73.7% |

**Table 5:** Confusion matrix of Physical (P) & Transportation (T) & Hand-related Activities (H).

**Free-Weight Exercises (E)**: Next, we evaluate the performance of our activity recognition scheme for recognizing free-weight exercises (E). We collected a total of 25 mins of data of five free-weight exercises from one subject. The performance is evaluated using leave-one-subject-out validation.

Table 6 shows the confusion matrix for the five free-weight exercises across seven subjects. As shown, BodyScan performs well in classifying these five exercises. Overall, it achieves an average recognition accuracy of 81.2% across these five activities. This result indicates that BodyScan has the potential of becoming a personal exercise tracking platform that identifies and records free-weight exercises.

| G/P | Bicep | Raise | Bent-over | Tricep | Chest |
|---|---|---|---|---|---|
| **Bicep** | 87.0% | 0.0% | 2.9% | 0.0% | 10.2% |
| **Raise** | 13.3% | 78.3% | 11.6% | 10.7% | 0.0% |
| **Bent-over** | 0.0% | 8.7% | 84.1% | 4.0% | 2.9% |
| **Tricep** | 0.0% | 17.4% | 6.7% | 73.9% | 0.0% |
| **Chest** | 15.9% | 0.0% | 1.4% | 0.0% | 82.6% |

**Table 6:** Confusion matrix of Free-Weight Exercises (E).

**Isolated Body Part Movements (I)**: Finally, we evaluate the performance of our activity recognition scheme for recognizing isolated body part movements (I). We collected a total of 36 mins of data from one subject. The performance is evaluated using leave-one-subject-out validation.

Table 7 shows the confusion matrix for the six isolated body part movements. Overall, BodyScan achieves an average recognition accuracy of 84.5%, indicating that BodyScan is capable of capturing and differentiating the six considered isolated body movements. When taking a closer look, we observe that *curl right arm* achieves the highest recall and the lowest precision among all the six body parts. In contrast, *curl left arm* achieves the lowest recall and the
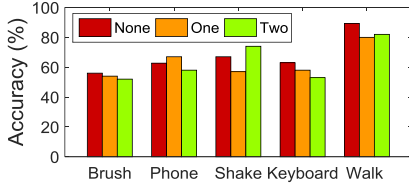
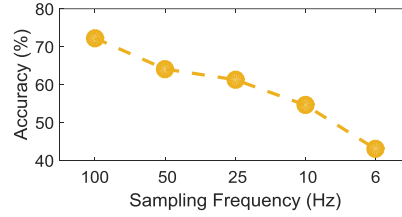**Figure 15:** Impact of interference of nearby people.
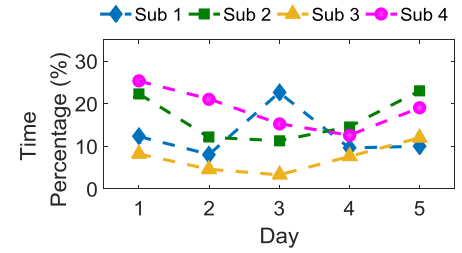


**Figure 16:** Impact of radio transmission rate.



**Figure 17:** Vital sign sensing opportunity in the field.

| G/P | CL | CR | SL | SR | SH | BO |
|-----|-----|-----|-----|-----|-----|-----|
| **CL** | 64.3% | 28.6% | 7.1% | 0.0% | 0.0% | 0.0% |
| **CR** | 0.0% | 100% | 0.0% | 0.0% | 0.0% | 0.0% |
| **SL** | 0.0% | 0.0% | 78.6% | 7.1% | 0.0% | 14.3% |
| **SR** | 0.0% | 14.3% | 0.0% | 85.7% | 0.0% | 0.0% |
| **SH** | 0.0% | 7.1% | 0.0% | 0.0% | 92.7% | 0.0% |
| **BO** | 0.0% | 0.0% | 14.3% | 0.0% | 0.0% | 85.7% |

**Table 7:** Confusion matrix of Isolated Body Part Movements (I). CL: *curl left arm*; CR: *curl right arm*; SL: *swing left leg*; SR: *swing right leg*; SH: *shake head*; BO: *bend over*.

highest precision. Recalling that the ESP wristband is worn on the left wrist and the HMB wearable unit is worn at the right hip, our observation implies that the performance of the isolated body movements are related to how close the body part is to the receiving antennas. This is because if the body part is closer to the receiving antennas, its intra-class variation can be more easily captured, resulting in a wider activity class boundary.

### 6.1.5 Impact of Radio Frequency Interference

In this experiment, we examine the impact of radio frequency interference (RFI) on the performance of activity recognition. Specifically, we used the clean environment with an average RFI value of 3.2 p/s as the baseline. In addition, we introduced extra RFI to create a noisy environment by setting up another radio transmission link at the same wireless channel using a TP-Link AC750 router and a laptop. Two RFI levels at 101.4 p/s and 214.3 p/s were created for our experiment. For both RFI levels and the baseline, we collected a total of 30 mins of data of five most common ADLs from one subject. The performance of BodyScan is evaluated using leave-one-trial-out validation.

Figure 13 illustrates the performance comparison between the clean and noisy environment. We observe that the activity recognition performance in general is jeopardized with the existence of RFI in the ambient environment. When taking a closer look, we find that RFI affects activities differently. Specifically, RFI has a more significant influence on the performance of activities that involve low-intensity body movements (i.e., *type on a phone*, *shake hands*, *type on a keyboard*) than those that involve high-intensity body movements (i.e., *walk*, *brush teeth*). This is because radio signals of activities with low-intensity body movements are more easily overshadowed by RFI.

### 6.1.6 Impact of Interference from Nearby People

Besides RFI, we also examine the impact of interference caused by nearby people on the performance of activity recognition. We examine three scenarios where we have zero, one, and two people staying within 1.2 to 2.1 meter range to the subject wearing BodyScan. During the experiment, one subject performs a total of 30 mins of data of five most common ADLs, while the people nearby performing some common activities such as speaking,

typing on the keyboard, and walking around. The performance of BodyScan is evaluated using leave-one-trial-out validation.

Figure 15 illustrates the performance comparison when zero, one, and two people are nearby. As shown, the recognition accuracies for different activities do not decrease in general when there are one or two people moving nearby. This result indicates that BodyScan is resilient to the interference caused by nearby people, validating the design choice of our conical horn directional antennas.

### 6.1.7 Impact of Radio Signal Transmission Rate

Next, we examine the impact of radio signal transmission rate on the performance of activity recognition. Specifically, we examine five transmission rates including 100 Hz, 50 Hz, 25 Hz, 10 Hz and 6 Hz. For the five transmission rates, we collected a total of 70 mins of data of the five most common ADLs from seven subjects. The performance of BodyScan at each transmission rate is evaluated using leave-one-subject-out validation.

Figure 16 illustrates the average recognition accuracies at all five transmission rates. The average recognition accuracies across all five activities and seven subjects are 72.3%, 64.1%, 61.3%, 54.6% and 43.0% at transmission rate of 100 Hz, 50 Hz, 25 Hz, 10 Hz and 6 Hz, respectively. The figure shows a clear trend that as the radio signal transmission rate decreases, the recognition accuracy drops. This result indicates that with the higher resolution provided by the higher transmission rate, our ECDF-based classification scheme can capture the shape of the distribution of each activity class more accurately. As such, the recognition performance is improved.

### 6.1.8 Impact of Antenna Configuration

Finally, we examine the impact of antenna configuration on the performance of activity recognition. Specifically, we examine five different antenna configurations: (1) dual upper-lower body directional antennas (UL) (our BodyScan design); (2) single upper body directional antenna (SU); (3) single lower body directional antenna (SL); (4) dual left-right body directional antennas (LR) (i.e., the dual directional antennas pointing to the left and right side of the human body); and (5) single omnidirectional antenna (SO). For five antenna configurations, we collected a total of 45 mins of data of the five most common ADLs from one subject. The performance of BodyScan is evaluated using leave-one-trial-out validation.

Table 8 lists the performance of all five antenna configurations. As shown, among all the five antenna configurations, UL achieves

| Antenna Configuration | Accuracy | Comment |
|-----|-----|-----|
| **UL** | 78.9% | Both upper and lower body antennas are considered |
| **SU** | 69.8% | Only upper body antenna is considered |
| **SL** | 56.0% | Only lower body antenna is considered |
| **LR** | 23.6% | Dual antennas point to left & right side of the body |
| **SO** | 50.3% | One antenna worn at the same body location as UL |

**Table 8:** Impact of antenna configuration.

| Processing Pipeline | 100 Hz | 50 Hz | 25 Hz | 10 Hz | 6 Hz |
|---|---|---|---|---|---|
| CSI Extraction | 0.702 | 0.596 | 0.354 | 0.278 | 0.134 |
| Preprocessing | 0.084 | 0.075 | 0.068 | 0.063 | 0.057 |
| Motion Detection | 0.083 | 0.064 | 0.046 | 0.035 | 0.028 |
| Breathing Rate Estimation | 0.182 | 0.167 | 0.146 | 0.138 | 0.122 |
| Activity Classification | 0.123 | 0.101 | 0.098 | 0.089 | 0.060 |
| Sensor Fusion | 0.001 | 0.001 | 0.001 | 0.001 | 0.001 |
| **Total (Breath Monitoring)** | 1.051 | 0.900 | 0.614 | 0.514 | 0.341 |
| **Total (Activity Recognition)** | 0.993 | 0.837 | 0.567 | 0.466 | 0.280 |

**Table 9:** Runtime performance of the radio signal processing pipeline at each stage measured on the HMB wearable unit. The processing time is measured in seconds.



(a) Power consumption of ESP.    (b) Power consumption of HMB.

**Figure 18:** Power consumption at different sampling frequencies.

| Device | 100 Hz | 70 Hz | 50 Hz | 25 Hz | 10 Hz | 6 Hz |
|---|---|---|---|---|---|---|
| ESP | 16.0 | 17.5 | 17.7 | 18.0 | 18.6 | 19.0 |
| HMB | 15.0 | 15.3 | 15.7 | 16.4 | 17.4 | 17.4 |

**Table 10:** Estimated battery lifetime of ESP wristband and HMB wearable unit under different sampling frequencies with the battery capacity of 700 mAh and 5000 mAh, respectively. The lifetime is measured in hours.

the best performance. This result is important because it validates the rationale behind the dual directional antenna design of BodyScan. In comparison, LR achieves the worst performance, with an average accuracy of only 23.6%. This is expected because with the dual directional antennas pointing toward the left and right side of the body, movements of upper and lower body caused by human activities can not be fully captured. We also observe that UL achieves better performance than SU and SL. This indicates that the activity recognition performance is improved if information from upper body and lower body movements are combined.

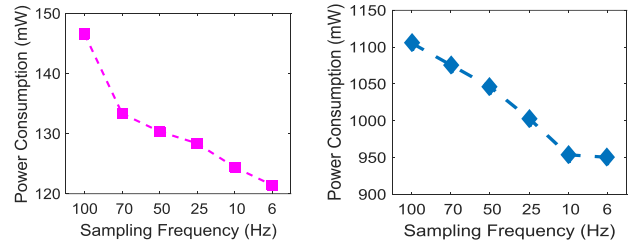## 6.2  System Performance

### 6.2.1  Experimental Setup

We examine the system performance of our BodyScan prototype in terms of runtime performance as well as power consumption and battery lifetime. To perform the evaluation, we set up the ESP wristband to continuously send radio signals and let the HMB wearable unit continuously receive radio signals. In addition, we implement the radio signal processing pipeline in the HMB wearable unit and run the pipeline on its 1.2 GHz ARM Cortex-A9 processor.

### 6.2.2  Runtime Performance

To examine the runtime performance of our BodyScan prototype, we measure the average processing time consumed at each stage of the radio signal processing pipeline at different CSI sampling frequencies. Specifically, we examine the runtime performance at the sampling frequency of 100 Hz, 50 Hz, 25 Hz, 10 Hz and 6 Hz, respectively. At each sampling frequency, we run 20 trials of a mix of different types of the targeted human activities from different subjects, with each trial containing five seconds of CSI data. We also run another 20 trials of breathing events from different subjects, with each trial containing 15 seconds of CSI data. We report the average processing time over 20 trials at each stage for human activity recognition and breath monitoring respectively in Table 9. The table shows that among all the processing stages, CSI extraction takes the most amount of time. It also shows that the processing time increases as the sampling frequency increases due to the increased number of CSI samples in each trial. More importantly, the table shows that even at the sampling frequency of 100 Hz, the total processing time for both activity recognition and breath monitoring is around one second. This indicates that with our lightweight radio signal processing pipeline design, our BodyScan prototype can achieve real-time performance.

### 6.2.3  Power Consumption and Battery Lifetime

To examine the power consumption of our BodyScan prototype, we use the Monsoon Power Monitor [8] to measure the power consumption of both the ESP wristband and the HMB wearable unit at the CSI sampling frequency of 100 Hz, 70 Hz, 50 Hz, 25 Hz, 12 Hz and 6 Hz, respectively. In order to save energy, we con-

figure both ESP wristband and HMB wearable unit to be at 50% duty cycle. At each sampling frequency, we measure the power consumption for 15 mins and report the average value in Figure 18. We also estimate the battery lifetimes of both ESP wristband and HMB wearable unit with the battery capacity of 700 mAh and 5000 mAh, respectively, assuming an ideal discharge curve of their batteries. Table 10 shows the estimated battery lifetimes at each sampling frequency. As shown, even at the sampling frequency of 100 Hz, our BodyScan prototype has an estimated battery lifetime of 15 hours. As users would not wear BodyScan continuously throughout the day (especially during sleep), the battery lifetime of our BodyScan prototype is sufficient for a daily usage with one single charge per day.

## 6.3  Deployment Study

### 6.3.1  Experimental Setup

**Subjects**: Four males out of the seven subjects we recruited volunteered to participate in the five-day deployment study.

**Experimental Environment**: The deployment study was conducted in real-world settings at subjects' homes and working places as well as in outdoor environment. The real-world environment is by no means clean from interference. Therefore, in our deployment study, we take into consideration both RFI and the interference caused by nearby people (i.e., people interference). In terms of RFI, we used WireShark to measure the RFI at places where target activities often occur. These include bedroom and bathroom at home, meeting room and corridor at working places as well as parking lot in outdoor environment. In terms of people interference, since it is impractical to accurately track the number of nearby people in the field, we used low, medium and high to provide a rough estimation of the level of people interference at different places.

**Data and Ground Truth Collection**: Throughout the five-day deployment study, the subjects were requested to wear the ESP wristband on the left wrist and the HMB wearable unit on the right hip and were encouraged to perform the target activities as much as they could. At the same time, they reserved the rights to take off BodyScan at any time when they did not feel comfortable of being monitored. To collect the ground truth, the subjects were asked to label the activities as well as to record the timestamps and places when the activities were performed. In total, 2499 mins of data

| Location | RFI | People Interference | Duration | Activity Recognition Performance |
|---|---|---|---|---|
| Meeting room 1 | 6.3 p/s | Medium | 12m | 54.1% |
| Meeting room 2 | 8.6 p/s | Medium | 14m | 59.1% |
| Bedroom | 14.0 p/s | Low | 10m | 67.5% |
| Bathroom | 8.3 p/s | Low | 2m | 78.3% |
| Parking Lot | 0.6 p/s | Low | 19m | 52.3% |
| Corridor | 7.5 p/s | High | 9m | 74.1% |
| Street | N/A | Low | 20m | 60.4% |

**Table 11:** Performance of activity recognition in the field (RFI of street is not available due to impracticality).

was collected from all four subjects during five days. However, a big portion of the collected data was either unlabeled or not belonging to the target activity categories. As such, only 86 mins of data was labeled.

### 6.3.2 Performance of Activity Recognition in the Field

Table 11 lists the activity recognition accuracies at different locations along with the corresponding average RFI values and people interference levels. The overall accuracy across all the seven locations is 60.2%. Given the challenging conditions in real-world settings, our result shows great promise of BodyScan as a practical solution for tracking a variety of human activities in the field. On the other hand, we also observe that the performance achieved in deployment study is worse than that achieved in controlled settings. One possible reason is that the orientation of the dual directional antennas was changed during data collection. As such, the antennas failed to capture the movements from both upper and lower body. Another possible reason that accounts for the worse performance is that more than one activity can be performed by the user simultaneously in the uncontrolled settings. For example, the user could type on the phone while walking. In such scenario, the collected radio signals contain mixed information from both activities, which is not covered by the activity model of BodyScan.

### 6.3.3 Vital Sign Sensing Opportunity in the Field

We are also interested in the feasibility of BodyScan for opportunistically sensing a user's vital sign information in real-world settings. Figure 17 shows the percentage of time in each day when the subjects' breathing rate information was captured by BodyScan during the deployment study. As shown, the average percentage of time over five days is 15.7%, 20.8%, 8.9% and 23.3% for each of the four subjects. This result indicates that BodyScan is capable of capturing breathing information for a reasonable amount of time in the uncontrolled real-world environment. It also demonstrates the great potential of BodyScan as a mobile health tool for monitoring an individual's breathing information in a non-intrusive manner.

### 6.3.4 Usability Study

Finally, at the end of the deployment study, we conduct a usability study on all four subjects by asking them to fill in a survey. The questions included in the survey are related to the comfortability, privacy, and safety of wearing BodyScan in real-world settings. We use the Likert Scale to code the answers of the subjects [33]. The Likert Scale adopts a five-point scale with points of -2 (strongly disagree), -1 (disagree), 0 (neutral), 1 (agree), and 2 (strongly agree).

Table 12 lists all the questions as well as the average and the standard deviation of the points calculated from the answers of all four subjects. In terms of comfortability, subjects in general feel comfortable when wearing BodyScan although their opinions vary significantly. In terms of privacy, subjects have a consensus that privacy is an issue they concern about in general. However, most subjects agree that they do not have a privacy concern about BodyScan. Finally, in terms of safety, subjects in general do not

worry about the radio exposure from BodyScan. Taken together, the results of the usability study show great potential of BodyScan to be adopted by users.

| Survey Questions | Mean | Standard Deviation |
|---|---|---|
| 1. User feels comfortable wearing BodyScan | 0.25 | 0.96 |
| 2. User concerns about privacy issues in general | 1.00 | 0.82 |
| 3. Radio sensing is not privacy-intrusive | 1.25 | 0.95 |
| 4. User does not worry about radio exposure | 0.50 | 0.58 |
| -2: Strongly Disagree, -1: Disagree, 0: Neutral, 1: Agree, 2: Strongly Agree | | |

**Table 12:** List of survey questions and survey results.

## 7. DISCUSSION AND FUTURE WORK

The experience of design and evaluation of BodyScan provides us with insights on both the promises and limitations of using radio as a sensor on wearable devices for human activity and vital sign monitoring. In this section, we elaborate on those insights in brief.

**Impact on Mobile and Wearable Sensing Systems:** BodyScan represents one of the pioneer explorations of transforming radio into an activity and vital sign sensor on wearable devices. In addition, one important element of the design of BodyScan is the correspondence of the form factor and the on-body locations with the smartphones and smartwatches/wristbands. With further research and optimization on both hardware platform and signal processing algorithms, we envision that the functionality of each component of BodyScan could be integrated into future generations of smartphones and wearables in the form of smartwatches, wristbands, or even eye glasses and cloth buttons. Given the prevalence of smartphones and the increasing popularity of wearables, as well as the new capabilities provided by radio-based sensing, we hope that this work could act as an enabler of inspiring new applications of smartphones and wearables in the areas such as mobile health, human-computer interaction, and social computing.

**Limitations on Activity Recognition:** BodyScan has made key strides in showing its feasibility in recognizing a rich and diverse set of human activities. However, it does not deliver perfect activity recognition performance mainly due to three limitations. First, it is possible that more than one activity can be performed by the user at the same time. In such case, the received radio signals contain mixed information from multiple activities, which is not covered by the activity model of BodyScan. Second, the activity recognition performance can be jeopardized if the dual directional antennas do not point to upper and lower body respectively. Since the wearable unit of our BodyScan prototype is still bulky, the orientation of the wearable unit is prone to be changed during usage. As such, the dual directional antennas may fail to capture the upper and lower body movements. We will work on miniaturizing the wearable unit to decrease its vulnerability to orientation change caused by its user. The third limitation is related to the tradeoff between computational complexity and real-time/power consumption performance. The resources of the current version of our BodyScan prototype are limited. To achieve real-time performance and to reduce power consumption, BodyScan sacrifices activity recognition performance by adopting computationally lightweight signal processing algorithms. We will work on improving the activity recognition performance by developing a new prototype with onboard dedicated low-power computational units (e.g., DSP) that can run complex algorithms efficiently.

**Limitations on Vital Sign Monitoring:** BodyScan is not able to provide accurate breathing rate estimation when the user is moving or performing activities that involve high-intensity body movements. This is because the intense body movements overshadow

the minute chest movements caused by inhaling and exhaling when breathing. Another limitation in the direction of vital sign monitoring is that BodyScan could not provide accurate heartbeat rate estimation even when the user is static or quasi-static (e.g., watching TV). This is due to the reason that movements caused by diastole and systole of heart beating are even more subtle compared to breathing. The signal-to-noise ratio (SNR) of the current version of our BodyScan system is not high enough to extract meaningful heartbeat information from the noise. We will work on improving the SNR of BodyScan from both hardware platform and signal processing algorithms perspectives with the objective to extract heartbeat information in the next version of BodyScan.

## 8. RELATED WORK

Our work is closely related to two research areas: (1) wearable and mobile sensing systems and (2) radio-based sensing systems.

**Mobile and Wearable Sensing Systems:** The past many years have witnessed the surge of smartphones and wearable devices. Powered by a variety of onboard sensors, these devices are capable of continuously monitoring users' behaviors as well as physiological signals in an ambulatory manner. Accelerometer, GPS, microphone and camera are the most popular sensors that have been extensively explored in the past. For example, accelerometer-based systems have been developed for hand gesture recognition [32], free weight exercise tracking [35], fall detection [28] and energy expenditure estimation [48]. GPS-based systems have been developed for transportation mode recognition [22, 39], social network identification [53] and personal environmental impact and exposure estimation [36]. Microphone-based systems have been developed for sleep quality monitoring [20], social interaction detection [26], vital sign sensing [38, 42], as well as eating and drinking behavior monitoring [27, 52, 23]. Finally, camera-based systems in the form of eye glasses or wearables worn around the neck have been developed for eye gaze tracking [34], shopping behavior monitoring [43] and lifelogging [45]. Different from all these existing systems, BodyScan explores using radio as a new sensing modality on wearable devices. It complements the existing sensing modalities of current wearable and mobile sensing systems by providing a contactless and privacy-preserving scheme to continuously monitor users' behavioral and physiological information.

**Radio-based Sensing Systems:** BodyScan is also related to radio-based sensing systems. Existing radio-based sensing systems can be primarily classified into software-defined radio (SDR) based and commercial off-the-shelf wireless device based systems. Pioneer work in radio-based sensing systems used high-cost SDRs combined with special hardware such as interference-nulling hardware and ultra-wideband radar transceivers to track human activities and vital signs. For example, WiSee uses Universal Software Radio Peripheral (USRP) SDR to enable whole-home sensing and recognition of human gestures [41]. WiTrack leverages Frequency Modulated Carrier Wave (FMCW) radar to track the 3D motion of a user [13]. Vital-Radio also uses FMCW but is designed to track the changes of radio signals caused by chest movements and skin vibrations to monitor breathing and heart rates [14].

To lower the costs incurred from SDRs and special hardware, systems based on commercial off-the-shelf wireless devices such as Wi-Fi routers and laptop computers with Wi-Fi cards have been developed. Many of these systems leveraged the fine-grained CSI measurements extracted from the radio signals to recognize activities that involve intense full body movements as well as activities that involve minute movements. For example, E-eyes uses CSI measurements to detect and recognize daily household activities

such as cooking and washing dishes [49]. WiFall leverages the time variability of the CSI measurements to detect accidental falls [19]. WiKey utilizes the unique patterns in the time-series of CSI measurements embedded in the minute movements of fingers and hands to recognize keystrokes [15].

BodyScan builds on the off-the-shelf wireless devices and the CSI-based scheme. However, the fundamental difference between the existing radio-based sensing systems and BodyScan is that existing systems use radio transmitters and receivers deployed in the ambient environment to sense human activities and physiological signals. In contrast, BodyScan utilizes radio transmitters and receivers in the form of wearables to achieve the same objective. In our recent work, we have developed a radio-based wearable sensing system called *HeadScan*, which uses a single pair of omnidirectional antennas worn on the shoulder and the collar respectively to capture head and mouth related activities including eating, drinking, speaking, and coughing [16]. In comparison, BodyScan adopts a different design by incorporating a pair of directional antennas with one pointing upward to detect upper body movements and the other pointing downward to detect lower body movements. Although the use of multiple antennas is a common practice in applications such as wireless localization [25], it is the first time this approach has been used for wearable radio-based sensing. Moreover, HeadScan employs a computationally expensive scheme based on sparse representation to process radio signals. In contrast, BodyScan utilizes lightweight schemes to realize on-device real-time radio signal processing.

## 9. CONCLUSION

In this paper, we presented the design, implementation and evaluation of BodyScan, a novel wearable system that uses radio alone to enable whole-body continuous sensing for human activity tracking and vital sign monitoring. Our prototype design of BodyScan comprises a pair of worn devices (wrist and hip placed); a design that corresponds to an increasingly common scenario where a user carries a smartphone while also wearing a wristband/smartwatch. Under controlled conditions, we find BodyScan – from just these two body positions – is able to recognize a wide range of activities (e.g., walk, ride a bike, shake hands, free-weight exercises) with promising accuracies and is able to estimate breathing rate with an average accuracy of 97.4%. Experiments under more realistic conditions show BodyScan can still achieve an average activity recognition accuracy above 60% and capture breathing information a reasonable amount of time each day. Through such results, BodyScan demonstrates the feasibility of radio-based wearable sensing. This is important because of the intrinsic benefits radio has over conventional mobile sensor modalities including more privacy preserving than a microphone or camera as well as requiring fewer body positions than an accelerometer for broad activity monitoring. For these reasons, we expect radio-based sensing to play an important role in the future evolution of wearable devices, and hope the design and techniques of BodyScan can act as a useful foundation for the subsequent investigations.

## 10. ACKNOWLEDGEMENT

# 11. REFERENCES

[1] Android Wear. https://www.android.com/wear/.

[2] Ansys HFSS. http://www.ansys.com/Products/Electronics/ANSYS-HFSS.

[3] Apple Watch. http://www.apple.com/watch/.

[4] Espressif ESP8266. http://www.espruino.com/EspruinoESP8266.

[5] Fitbit Activity Tracker. https://www.fitbit.com/.

[6] HummingBoard Pro. http://wiki.solid-run.com/doku.php?id=products:imx6:hummingboard.

[7] Intel 5300. http://www.intel.com/content/www/us/en/wireless-products/ultimate-n-wifi-link-5300-brief.html.

[8] Monsoon Power Monitor. http://www.msoon.com/LabEquipment/PowerMonitor/.

[9] NeuLog Respiration Monitor Belt Logger Sensor. https://neulog.com/.

[10] Samsung Wearables. http://www.samsung.com/us/mobile/wearable-tech.

[11] Wearable device market value from 2010 to 2018. http://www.statista.com/statistics/259372/wearable-device-market-value/.

[12] WireShark. https://www.wireshark.org/.

[13] F. Adib, Z. Kabelac, D. Katabi, and R. Miller. 3d tracking via body radio reflections. In *Usenix NSDI*, volume 14, 2014.

[14] F. Adib, H. Mao, Z. Kabelac, D. Katabi, and R. Miller. Smart homes that monitor breathing and heart rate. In *Proceedings of the 33rd Annual ACM Conference on Human Factors in Computing Systems*, pages 837–846. ACM, 2015.

[15] K. Ali, A. X. Liu, W. Wang, and M. Shahzad. Keystroke recognition using wifi signals. In *Proceedings of the 21st Annual International Conference on Mobile Computing and Networking*, pages 90–102. ACM, 2015.

[16] B. Fang, N. D. Lane, M. Zhang, and F. Kawsar. Headscan: A wearable system for radio-based sensing of head and mouth-related activities. In *Proceedings of the 15th ACM/IEEE International Conference on Information Processing in Sensor Networks (IPSN)*, 2016.

[17] D. Halperin, W. Hu, A. Sheth, and D. Wetherall. Tool release: Gathering 802.11n traces with channel state information. *ACM SIGCOMM CCR*, 41(1):53, Jan. 2011.

[18] N. Y. Hammerla, R. Kirkham, P. Andras, and T. Ploetz. On preserving statistical characteristics of accelerometry data using their empirical cumulative distribution. In *Proceedings of the 2013 International Symposium on Wearable Computers*, pages 65–68. ACM, 2013.

[19] C. Han, K. Wu, Y. Wang, and L. M. Ni. Wifall: Device-free fall detection by wireless networks. In *INFOCOM, 2014 Proceedings IEEE*, pages 271–279. IEEE, 2014.

[20] T. Hao, G. Xing, and G. Zhou. isleep: unobtrusive sleep quality monitoring using smartphones. In *Proceedings of the 11th ACM Conference on Embedded Networked Sensor Systems*, page 4. ACM, 2013.

[21] J. Heiskala and J. Terry. *OFDM wireless LANs: A theoretical and practical guide*. Sams, 2001.

[22] S. Hemminki, P. Nurmi, and S. Tarkoma. Accelerometer-based transportation mode detection on smartphones. In *Proceedings of the 11th ACM Conference on Embedded Networked Sensor Systems*, SenSys '13, pages 13:1–13:14, New York, NY, USA, 2013. ACM.

[23] Y. Ju, Y. Lee, J. Yu, C. Min, I. Shin, and J. Song. Symphoney: A coordinated sensing flow execution engine for concurrent mobile sensing applications. In *Proceedings of the 10th ACM Conference on Embedded Network Sensor Systems*, SenSys '12, pages 211–224, New York, NY, USA, 2012. ACM.

[24] N. Karakayali. Social distance and affective orientations. In *Sociological Forum*, volume 23, 2009.

[25] K. Kleisouris, Y. Chen, J. Yang, and R. P. Martin. The impact of using multiple antennas on wireless localization. In *Sensor, Mesh and Ad Hoc Communications and Networks, 2008. SECON'08. 5th Annual IEEE Communications Society Conference on*, pages 55–63. IEEE, 2008.

[26] Y. Lee, C. Min, C. Hwang, J. Lee, I. Hwang, Y. Ju, C. Yoo, M. Moon, U. Lee, and J. Song. Sociophone: Everyday face-to-face interaction monitoring platform using multi-phone sensor fusion. In *Proceeding of the 11th annual international conference on Mobile systems, applications, and services*, pages 375–388. ACM, 2013.

[27] Y. Lee, C. Min, C. Hwang, J. Lee, I. Hwang, Y. Ju, C. Yoo, M. Moon, U. Lee, and J. Song. Sociophone: Everyday face-to-face interaction monitoring platform using multi-phone sensor fusion. In *Proceeding of the 11th Annual International Conference on Mobile Systems, Applications, and Services*, MobiSys '13, pages 375–388, New York, NY, USA, 2013. ACM.

[28] Q. Li, J. A. Stankovic, M. A. Hanson, A. T. Barth, J. Lach, and G. Zhou. Accurate, fast fall detection using gyroscopes and accelerometer-derived posture information. In *Wearable and Implantable Body Sensor Networks, 2009. BSN 2009. Sixth International Workshop on*, pages 138–143. IEEE, 2009.

[29] Y. Li, L. J. Cimini Jr, and N. R. Sollenberger. Robust channel estimation for ofdm systems with rapid dispersive fading channels. *Communications, IEEE Transactions on*, 46(7):902–915, 1998.

[30] W. Lindh, M. Pooler, C. Tamparo, B. Dahl, and J. Morris. *Delmarq́s comprehensive medical assisting: administrative and clinical competencies*. Cengage Learning, 2013.

[31] J. Liu, Y. Wang, Y. Chen, J. Yang, X. Chen, and J. Cheng. Tracking vital signs during sleep leveraging off-the-shelf wifi. In *Proceedings of the 16th ACM International Symposium on Mobile Ad Hoc Networking and Computing*, pages 267–276. ACM, 2015.

[32] J. Liu, L. Zhong, J. Wickramasuriya, and V. Vasudevan. uwave: Accelerometer-based personalized gesture recognition and its applications. *Pervasive and Mobile Computing*, 5(6):657–675, 2009.

[33] T. J. Maurer and H. R. Pierce. A comparison of likert scale and traditional measures of self-efficacy. *Journal of applied psychology*, 83(2):324, 1998.

[34] A. Mayberry, P. Hu, B. Marlin, C. Salthouse, and D. Ganesan. ishadow: Design of a wearable, real-time mobile gaze tracker. In *Proceedings of the 12th Annual International Conference on Mobile Systems, Applications, and Services*, MobiSys '14, pages 82–94, New York, NY, USA, 2014. ACM.

[35] D. Morris, T. S. Saponas, A. Guillory, and I. Kelner. Recofit: using a wearable sensor to find, recognize, and count repetitive exercises. In *Proceedings of the SIGCHI Conference on Human Factors in Computing Systems*, pages 3225–3234. ACM, 2014.

[36] M. Mun, S. Reddy, K. Shilton, N. Yau, J. Burke, D. Estrin, M. Hansen, E. Howard, R. West, and P. Boda. Peir, the personal environmental impact report, as a platform for participatory sensing systems research. In *Proceedings of the 7th international conference on Mobile systems, applications, and services*, pages 55–68. ACM, 2009.

[37] R. Nandakumar, B. Kellogg, and S. Gollakota. Wi-fi gesture recognition on existing devices. *arXiv preprint arXiv:1411.5394*, 2014.

[38] S. Nirjon, R. F. Dickerson, Q. Li, P. Asare, J. A. Stankovic, D. Hong, B. Zhang, X. Jiang, G. Shen, and F. Zhao. Musicalheart: A hearty way of listening to music. In *Proceedings of the 10th ACM Conference on Embedded Network Sensor Systems*, pages 43–56. ACM, 2012.

[39] D. Patterson, L. Liao, D. Fox, and H. Kautz. Inferring high-level behavior from low-level sensors. In *UbiComp 2003: Ubiquitous Computing*, pages 73–89. Springer, 2003.

[40] J. Platt et al. Probabilistic outputs for support vector machines and comparisons to regularized likelihood methods. *Advances in large margin classifiers*, 10(3):61–74, 1999.

[41] Q. Pu, S. Gupta, S. Gollakota, and S. Patel. Whole-home gesture recognition using wireless signals. In *Proceedings of the 19th annual international conference on Mobile computing & networking*, pages 27–38. ACM, 2013.

[42] T. Rahman, A. T. Adams, M. Zhang, E. Cherry, B. Zhou, H. Peng, and T. Choudhury. Bodybeat: A mobile system for sensing non-speech body sounds. In *Proceedings of the 12th Annual International Conference on Mobile Systems, Applications, and Services*, MobiSys '14, pages 2–13, New York, NY, USA, 2014. ACM.

[43] S. Rallapalli, A. Ganesan, K. Chintalapudi, V. Padmanabhan, and L. Qiu. Enabling physical analytics in retail stores using smart glasses. In *Proceedings of the 20th annual international conference on Mobile computing and networking*, pages 115–126. ACM, 2014.

[44] A. Rodríguez-Molinero, L. Narvaiza, J. Ruiz, and C. Gálvez-Barrón. Normal respiratory rate and peripheral blood oxygen saturation in the elderly population. *Journal of the American Geriatrics Society*, 61(12):2238–2240, 2013.

[45] A. Sellen, A. Fogg, M. Aitken, S. Hodges, C. Rother, and K. Wood. Do life-logging technologies support memory for the past?: an experimental study using sensecam. In *Proceedings of the SIGCHI conference on Human factors in computing systems*, pages 81–90. ACM, 2007.

[46] P. Stoica and R. Moses. *Introduction to spectral analysis*, volume 1. Prentice hall Upper Saddle River, 1997.

[47] A. W. Van der Vaart. *Asymptotic statistics*, volume 3. Cambridge university press, 2000.

[48] H. Vathsangam, M. Zhang, A. Tarashansky, A. A. Sawchuk, and G. Sukhatme. Towards practical energy expenditure estimation with mobile phones. In *Signals, Systems and Computers, 2013 Asilomar Conference on*, pages 74–79. IEEE, 2013.

[49] Y. Wang, J. Liu, Y. Chen, M. Gruteser, J. Yang, and H. Liu. E-eyes: device-free location-oriented activity identification using fine-grained wifi signatures. In *Proceedings of the 20th annual international conference on Mobile computing and networking*, pages 617–628. ACM, 2014.

[50] B. Wei, W. Hu, M. Yang, and C. T. Chou. Radio-based device-free activity recognition with radio frequency interference. In *Proceedings of the 14th International Conference on Information Processing in Sensor Networks*, IPSN '15, pages 154–165, New York, NY, USA, 2015. ACM.

[51] C. Wu, Z. Yang, Z. Zhou, X. Liu, Y. Liu, and J. Cao. Non-invasive detection of moving and stationary human with wifi. *Selected Areas in Communications, IEEE Journal on*, 33(11):2329–2342, 2015.

[52] K. Yatani and K. N. Truong. Bodyscope: A wearable acoustic sensor for activity recognition. In *Proceedings of the 2012 ACM Conference on Ubiquitous Computing*, UbiComp '12, pages 341–350, New York, NY, USA, 2012. ACM.

[53] Y. Zheng, Y. Chen, X. Xie, and W.-Y. Ma. Geolife2. 0: a location-based social networking service. In *Mobile Data Management: Systems, Services and Middleware, 2009. MDM'09. Tenth International Conference on*, pages 357–358. IEEE, 2009.